

Radiation Effect on MHD Flow Past an Inclined Plate with Variable Temperature and Mass Diffusion

U. S. Rajput and Gaurav Kumar*

Department of Mathematics and Astronomy, University of Lucknow, India

Abstract: The present study is carried out to examine the effects of radiation and Hall current on unsteady natural convection flow of a viscous, incompressible and electrically conducting fluid past an impulsively started inclined plate under the influence of transversely applied uniform magnetic field. The governing equations involved in the present analysis are solved by the Laplace-transform technique. The results obtained are discussed with the help of graphs drawn for different parameters like thermal Grashof number, mass Grashof number, Prandtl number, Hall current parameter, radiation parameter, magnetic field parameter and Schmidt number. The numerical values obtained for skin-friction and Nusselt number have been tabulated. The results obtained are in agreement with the actual flow phenomenon. The motive of this study is to analyze radiation and the Hall effect on the flow model. In the study, we found that the velocity in the boundary layer increases with the values of radiation and Hall current parameters. It is also observed that radiation and the Hall current increase the drag at the plate surface.

Keywords: MHD flow; inclined plate; radiation effect; variable temperature; mass diffusion; Hall current.

1. Introduction

The study of MHD flow with heat and mass transfer plays important role in different areas of science and technology like chemical engineering, mechanical engineering, petroleum engineering, biomechanics, irrigation engineering and aerospace technology. The study of radiation and Hall effects on MHD flow is also significant in many cases. Some problems related to radiation effect are mentioned here. Radiation effect on free convection flow past a semi-infinite vertical plate was analyzed by Soundalgekar and Takhar [1]. Hall effect on magnetohydrodynamic boundary layer flow over a continuous moving flat plate was studied by Pop and Watanabe [2]. Radiation effect on mixed convection along a vertical plate with uniform surface temperature was considered by Hossain and Takhar [3]. Takhar *et al.* [4] have analyzed radiation effect on MHD free convection flow of a radiating gas past a semi-infinite vertical plate. Raptis and Massals [5] have investigated magnetohydrodynamics flow past a plate in the presence of radiation. Raptis along with Perdikis [6] have worked on radiation and free convection flow past a moving plate. Radiative free convective non-Newtonian fluid flow past a wedge embedded in a porous medium was studied by Chamkha *et al.* [7]. Mebine [8] has investigated radiation effect on MHD Couette flow with heat transfer between two parallel plates. Radiation and mass transfer effects on the magnetohydrodynamic unsteady flow induced by a stretching sheet was investigated by Hayat *et al.* [9]. Combined effects of MHD and radiation on unsteady transient free convection flow

*Corresponding author; e-mail: rajputgauravlko@gmail.com
doi: 10.6703/IJASE.2017.14(3).171
©2017 Chaoyang University of Technology, 1727-2394

Received 24 February 2016
Revised 27 July 2016
Accepted 28 February 2017

between two long vertical parallel plates with constant temperature and mass diffusion was studied by Rajput and Sahu [10]. Rani *et al.* [11] have developed Hall current effect on convective heat and mass transfer flow of viscous fluid in a vertical wavy channel. Aligned magnetic field, radiation and rotation effects on unsteady hydromagnetic free convection flow past an impulsively moving vertical plate in a porous medium was presented by Sandeep *et al.* [12]. Sandeep *et al.* [13] have discussed radiation and inclined magnetic field effects on unsteady MHD convective flow past an impulsively moving vertical plate in a porous medium. Recently many others researchers [14-18] analyzed the effect of radiation effect on MHD flow past an impulsively started vertical plate with heat and mass transfer. Reddy *et al.* [19] have approached thermo diffusion and Hall current effects on an unsteady flow of a nano fluid under the influence of inclined magnetic field. We are considering the radiation effect on unsteady MHD flow past an impulsively started inclined plate with variable temperature and mass diffusion in the presence of Hall current. The results are shown with the help of graphs and table.

2. Mathematical Analysis

The geometric model of the problem is shown in Figure 1. The x axis is taken along the plane and z normal to it. The plate is inclined at angle α from vertical. A transverse magnetic field B_0 of uniform strength is applied on the flow. During the motion, the direction of the magnetic field changes along with the plate in such a way that it always remains perpendicular to it. This means, the magnetic field is stationary with the plate. Initially it has been considered that the plate as well as the fluid is at the same temperature T_∞ . The species concentration in the fluid is taken as C_∞ . At time $t > 0$, the plate starts moving with a velocity u_0 in its own plane, and temperature of the plate is raised to T_w . The concentration C near the plate is raised linearly with respect to time.

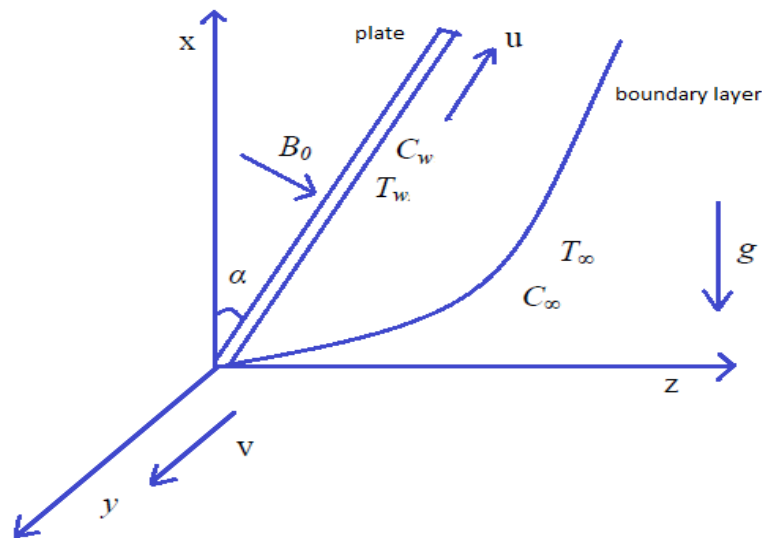


Figure 1. Geometric model

The flow modal is as under:

$$\frac{\partial u}{\partial t} = \nu \frac{\partial^2 u}{\partial z^2} + g\beta \cos \alpha (T - T_\infty) + g\beta^* \cos \alpha (C - C_\infty) - \frac{\sigma B_0^2 (u + mv)}{\rho(1 + m^2)} \quad (1)$$

$$\frac{\partial v}{\partial t} = \nu \frac{\partial^2 v}{\partial z^2} + \frac{\sigma B_0^2 (mu - v)}{\rho(1 + m^2)} \quad (2)$$

$$\frac{\partial C}{\partial t} = D \frac{\partial^2 C}{\partial z^2} \quad (3)$$

$$\rho C_p \frac{\partial T}{\partial t} = k \frac{\partial^2 T}{\partial z^2} - \frac{\partial q_r}{\partial z} \quad (4)$$

The corresponding initial and boundary conditions are

$$\left. \begin{aligned} t \leq 0 : u = 0, v = 0, T = T_\infty, C = C_\infty, \quad \text{for all } z, \\ t > 0 : u = u_0, v = 0, T = T_\infty + (T_w - T_\infty) \frac{u_0^2 t}{\nu}, C = C_\infty + (C_w - C_\infty) \frac{u_0^2 t}{\nu}, \quad \text{at } z=0, \\ u \rightarrow 0, v \rightarrow 0, T \rightarrow T_\infty, C \rightarrow C_\infty \quad \text{as } z \rightarrow \infty. \end{aligned} \right\} \quad (5)$$

Here u is the primary velocity, v -the secondary velocity, g -the acceleration due to gravity, β -volumetric coefficient of thermal expansion, t -time, $m (= \omega_e \tau_e)$ is the Hall current parameter with ω_e -cyclotron frequency of electrons and τ_e -electron collision time, T -temperature of the fluid, β^* -volumetric coefficient of concentration expansion, C -species concentration in the fluid, ν -the kinematic viscosity, ρ -the density, C_p -the specific heat at constant pressure, k -thermal conductivity of the fluid, D -the mass diffusion coefficient, T_w -temperature of the plate at $z = 0$, C_w -species concentration at the plate $z = 0$, B_0 -the uniform magnetic field, and σ - the electrical conductivity.

The local radiant for the case of an optically thin gray gas is expressed by

$$\frac{\partial q_r}{\partial z} = -4a^* \sigma (T_\infty^4 - T^4) \quad (6)$$

where a^* is absorption constant. Considering the temperature difference within the flow sufficiently small, T^4 can be expressed as the linear function of temperature. This is accomplished by expanding T^4 in a Taylor series about T_∞ and neglecting higher-order terms.

$$T^4 \cong 4T_\infty^3 T - 3T_\infty^4 \quad (7)$$

Using equations (6) and (7), equation (4) becomes

$$\rho C_p \frac{\partial T}{\partial t} = k \frac{\partial^2 T}{\partial z^2} - 16a^* \sigma T_\infty^3 (T - T_\infty) \quad (8)$$

The following non-dimensional quantities are introduced to transform equations (1), (2), (3) and (8) into dimensionless form:

$$\left. \begin{aligned} \bar{z} &= \frac{zu_0}{v}, \bar{u} = \frac{u}{u_0}, \bar{v} = \frac{v}{u_0}, \theta = \frac{(T-T_\infty)}{(T_w-T_\infty)}, S_c = \frac{v}{D}, \mu = \rho v, P_r = \frac{\mu c_p}{k}, R = \frac{16a^* \sigma v^2 T_\infty^3}{ku_0^2}, \\ G_r &= \frac{g\beta v(T_w-T_\infty)}{u_0^3}, M = \frac{\sigma B_0^2 v}{\rho u_0^2}, G_m = \frac{g\beta^* v(C_w-C_\infty)}{u_0^3}, \bar{C} = \frac{(C-C_\infty)}{(C_w-C_\infty)}, \bar{t} = \frac{tu_0^2}{v}. \end{aligned} \right\} \quad (9)$$

Here \bar{u} is the dimensionless primary velocity, \bar{v} -the secondary velocity, \bar{t} -dimensionless time, θ -the dimensionless temperature, \bar{C} -the dimensionless concentration, G_r -thermal Grashof number, G_m - mass Grashof number, μ -the coefficient of viscosity, R -Radiation parameter, P_r -the Prandtl number, S_c -the Schmidt number, and M -the magnetic parameter. Thus the model becomes

$$\frac{\partial \bar{u}}{\partial \bar{t}} = \frac{\partial^2 \bar{u}}{\partial \bar{z}^2} + G_r \cos \alpha \theta + G_m \cos \alpha \bar{C} - \frac{M(\bar{u} + m\bar{v})}{(1+m^2)} \quad (10)$$

$$\frac{\partial \bar{v}}{\partial \bar{t}} = \frac{\partial^2 \bar{u}}{\partial \bar{z}^2} + \frac{M(m\bar{u} - \bar{v})}{(1+m^2)} \quad (11)$$

$$\frac{\partial \bar{C}}{\partial \bar{t}} = \frac{1}{S_c} \frac{\partial^2 \bar{C}}{\partial \bar{z}^2} \quad (12)$$

$$\frac{\partial \theta}{\partial \bar{t}} = \frac{1}{P_r} \frac{\partial^2 \theta}{\partial \bar{z}^2} - \frac{R\theta}{P_r} \quad (13)$$

The corresponding boundary conditions become

$$\left. \begin{aligned} \bar{t} \leq 0 : \bar{u} = 0, \bar{v} = 0, \theta = 0, \bar{C} = 0, & \quad \text{for all } \bar{z}, \\ \bar{t} > 0 : \bar{u} = 1, \bar{v} = 0, \theta = \bar{t}, \bar{C} = \bar{t}, & \quad \text{at } \bar{z} = 0, \\ \bar{u} \rightarrow 0, \bar{v} \rightarrow 0, \theta \rightarrow 0, \bar{C} \rightarrow 0, & \quad \text{as } \bar{z} \rightarrow \infty \end{aligned} \right\} \quad (14)$$

Dropping bars in the above equations, we get

$$\frac{\partial u}{\partial t} = \frac{\partial^2 u}{\partial z^2} + G_r \cos \alpha \theta + G_m \cos \alpha C - \frac{M(u + mv)}{(1+m^2)}, \quad (15)$$

$$\frac{\partial v}{\partial t} = \frac{\partial^2 v}{\partial z^2} + \frac{M(mu - v)}{(1+m^2)}, \quad (16)$$

$$\frac{\partial C}{\partial t} = \frac{1}{S_c} \frac{\partial^2 C}{\partial z^2}, \quad (17)$$

$$\frac{\partial \theta}{\partial t} = \frac{1}{P_r} \frac{\partial^2 \theta}{\partial z^2} - \frac{R\theta}{P_r}. \quad (18)$$

The boundary conditions are

$$\left. \begin{aligned} t \leq 0 : u = 0, v = 0, \theta = 0, C = 0, & \quad \text{for all } z, \\ t > 0 : u = 1, v = 0, \theta = t, C = t, & \quad \text{at } z = 0, \\ u \rightarrow 0, v \rightarrow 0, \theta \rightarrow 0, C \rightarrow 0, & \quad \text{as } z \rightarrow \infty \end{aligned} \right\} \quad (19)$$

Combining equations (15) and (16), the model becomes

$$\frac{\partial q}{\partial t} = \frac{\partial^2 q}{\partial z^2} + G_r \text{Cosa } \theta + G_m \text{Cosa } C - qa, \quad (20)$$

$$\frac{\partial C}{\partial t} = \frac{1}{S_c} \frac{\partial^2 C}{\partial z^2}, \quad (21)$$

$$\frac{\partial \theta}{\partial t} = \frac{1}{P_r} \frac{\partial^2 \theta}{\partial z^2} - \frac{R\theta}{P_r}. \quad (22)$$

Finally, the boundary conditions become:

$$\left. \begin{aligned} t \leq 0 : q = 0, \theta = 0, C = 0, & \quad \text{for all } z, \\ t > 0 : q = 1, \theta = t, C = t, & \quad \text{at } z = 0, \\ q \rightarrow 0, \theta \rightarrow 0, C \rightarrow 0, & \quad \text{as } z \rightarrow \infty. \end{aligned} \right\} \quad (23)$$

Here $q = u + i v$, $a = \frac{M(1 - im)}{1 + m^2}$.

The dimensionless governing equations (20) to (22), subject to the boundary conditions (23), are solved by the usual Laplace - transform technique. The solution obtained is as under:

$$\begin{aligned} C &= t \left\{ \left(1 + \frac{z^2 S_c}{2t} \right) \text{erfc} \left[\frac{\sqrt{S_c}}{2\sqrt{t}} \right] - \frac{z\sqrt{S_c}}{\sqrt{\pi}\sqrt{t}} e^{-\frac{z^2}{4t} S_c} \right\}, \\ \theta &= \frac{e^{-\sqrt{R}z}}{4\sqrt{R}} \left\{ \text{erfc} \left[\frac{-2\sqrt{R}t + zP_r}{\sqrt{P_r t}} \right] (2\sqrt{R}t - zR) + e^{2\sqrt{R}z} \text{erfc} \left[\frac{2\sqrt{R}t + zP_r}{\sqrt{P_r t}} \right] (2\sqrt{R}t + zR) \right\}, \\ q &= \frac{1}{2} e^{-\sqrt{a}z} A_{33} + \frac{G_r \text{Cosa} \alpha}{4(a-R)^2} [2e^{-\sqrt{a}z} (A_1 + P_r A_2) + 2t A_2 e^{-\sqrt{a}z} (a-R) + z A_3 e^{-\sqrt{a}z} (\sqrt{a} - \frac{R}{\sqrt{a}}) + 2A_{12} A_4 (1 - P_r)] + \\ &\quad \frac{G_m \text{Cosa} \alpha}{4a^2} [e^{-\sqrt{a}z} (2A_1 + 2\sqrt{a} A_3) + 2e^{-\sqrt{a}z} A_2 (S_c + at) + 2A_{13} A_5 (1 - S_c)] - \frac{P_r G_r \text{Cosa} \alpha}{2\sqrt{\pi} (a-R)^2 A_{11}} [A_{16} A_6 \sqrt{\pi} z (at - 1 \\ &\quad - Rt + P_r) + A_{14} A_7 \sqrt{\pi} z (1 - P_r) + \frac{1}{2\sqrt{R/P_r}} A_{16} A_8 A_{11} \sqrt{\pi} z (a-R)] - \frac{G_m \text{Cosa} \alpha}{2a^2 \sqrt{\pi}} [2az \sqrt{S_c} e^{-\frac{z^2 S_c}{4t}} \sqrt{t} + A_{15} \sqrt{\pi} (az^2 S_c \\ &\quad + 2at + 2S_c - 2) + A_{13} \sqrt{\pi} (A_9 + A_{10} S_c)] \end{aligned}$$

The expressions for the constants involved in the solution are given in the appendix.

Skin Friction: the dimensionless skin friction at the plate $z=0$ is obtained by

$$\left(\frac{dq}{dz} \right)_{z=0} = \tau_x + i \tau_y.$$

Nusselt Number: the dimensionless Nusselt number at the plate $z=0$ is given by

$$Nu = \left(\frac{\partial \theta}{\partial z} \right)_{z=0} = \text{erfc} \left[\frac{\sqrt{R}t}{\sqrt{tP_r}} \right] (\sqrt{R}t - \frac{\sqrt{R}}{2} t + \frac{P_r}{4\sqrt{R}}) - \text{erfc} \left[-\frac{\sqrt{R}t}{\sqrt{tP_r}} \right] \left(\frac{\sqrt{R}}{2} t + \frac{P_r}{4\sqrt{R}} \right) - \frac{e^{-\frac{Rt}{P_r}} \sqrt{tP_r}}{\sqrt{\pi}}.$$

3. Result and Discussions

The velocity profiles for different parameters like thermal Grashof number (Gr), magnetic field (M), Hall parameter (m), radiation (R), Prandtl number (Pr) and time (t) are shown from Figures 2 to 19. Temperature profiles for different values of (Pr), (R) and time are shown in Figures 20 to 22. It is observed from Figures 2 and 11 that the primary and secondary velocities of fluid decrease when the angle of inclination (α) is increased. This is in agreement with the actual flow, since the velocity of the fluid must decrease with the increase of the inclination of the plate from vertical. Figures 3, 4, 12 and 13 show the buoyancy effect. It is observed that both the primary and secondary velocities increase on increasing thermal Grashof number (Gr) and mass Grashof number (Gm). This indicates that buoyancy force in the boundary layer region near the plate tends to accelerate primary and secondary velocities. Also, if Hall current parameter m is increased then u increases, while v gets decreased (Figures 5 and 14). It is observed from Figures 6 and 15 that the effect of increasing values of the parameter (M) results in decreasing u and increasing v . It is in agreement since the magnetic field establishes a force which acts against the main flow resulting in slowing down the velocity of fluid. It is deduced that when radiation parameter (R) is increased then the velocities are increased (Figures 7 and 16). Further, it is observed that velocities decrease when Prandtl number and Schmidt number are increased (Figures 8, 9, 17 and 18). In actual sense, the increase of Sc means decrease of molecular diffusivity (D). This shows that the process of diffusion will decrease. Further, from Figures 10 and 19, it is observed that velocities increase with time. It is observed that temperature decreases when Prandtl number and radiation parameter are increased (Figures 20 and 21). However, from Figure 22 it is observed that temperature increases with time.

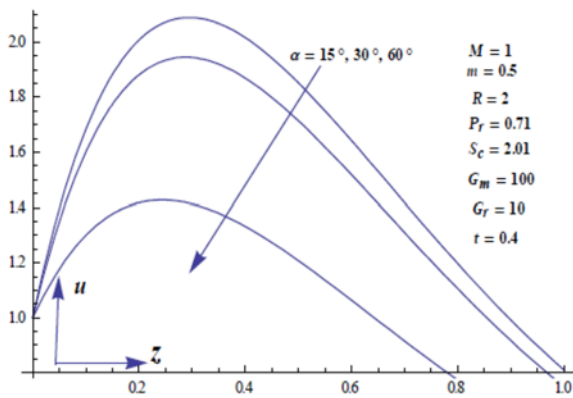


Figure 2. Velocity u for different values of α

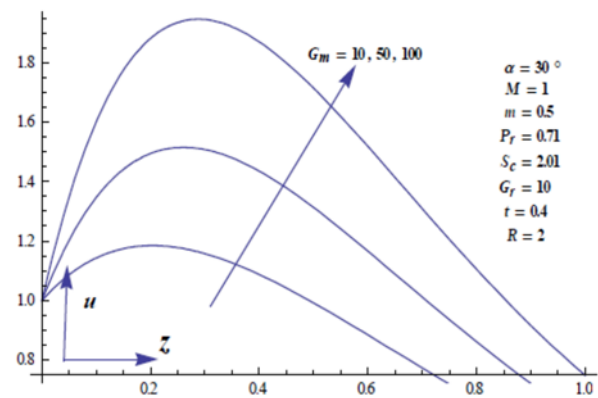


Figure 3. Velocity u for different values of Gm

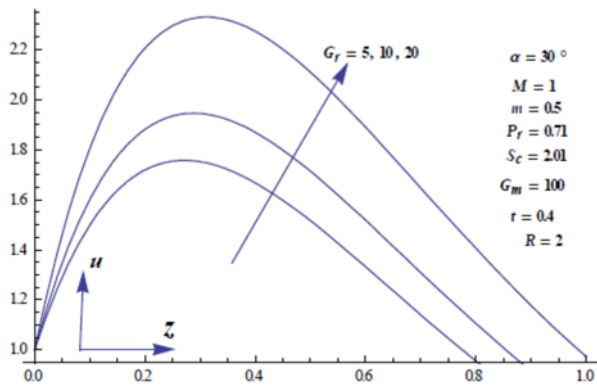


Figure 4. Velocity u for different values of Gr

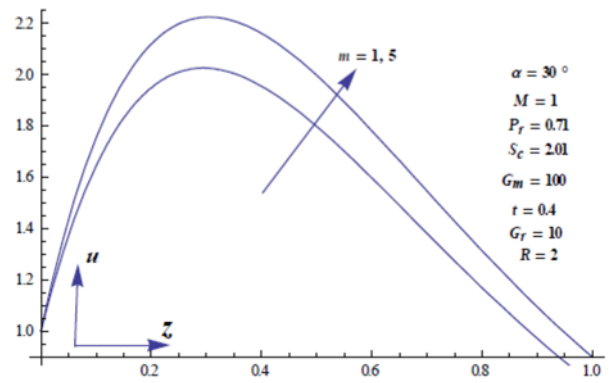


Figure 5. Velocity u for different values of m

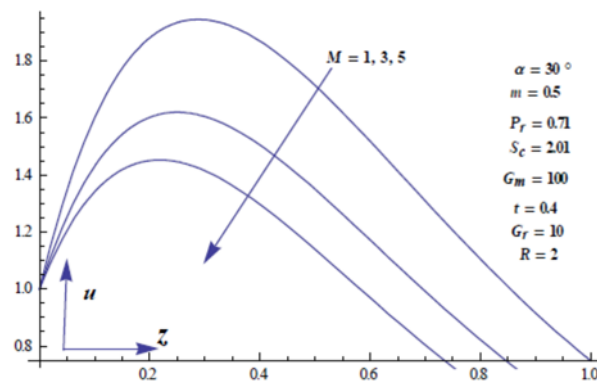


Figure 6. Velocity u for different values of M

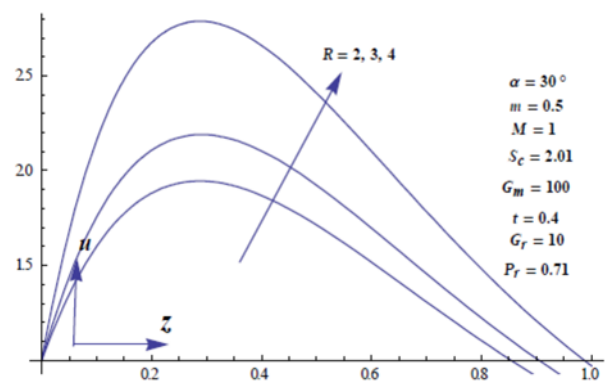


Figure 7. Velocity u for different values of R

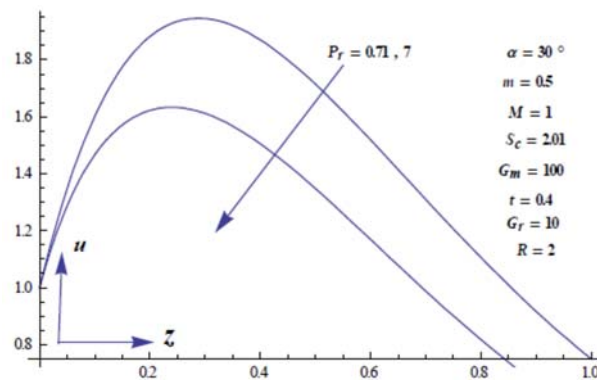


Figure 8. Velocity u for different values of Pr

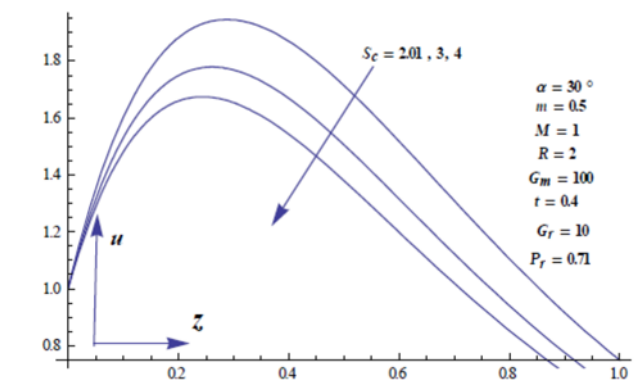


Figure 9. Velocity u for different values of Sc

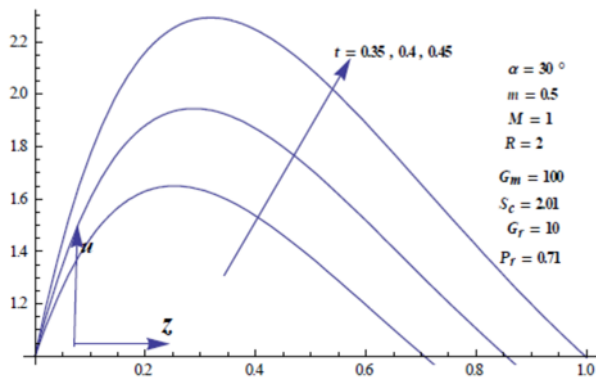


Figure 10. Velocity u for different values of t

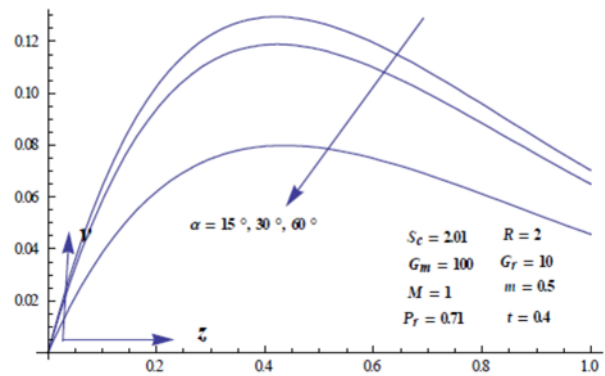


Figure 11. Velocity v for different values of α

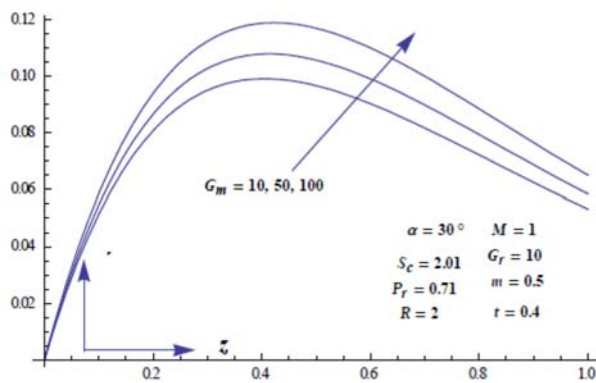


Figure 12. Velocity v for different values of Gm

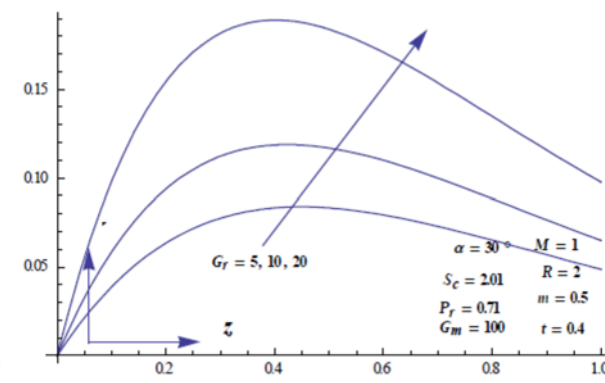


Figure 13. Velocity v for different values of Gr

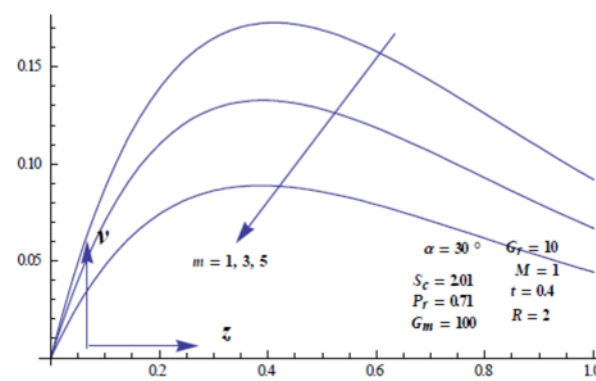


Figure 14. Velocity v for different values of m

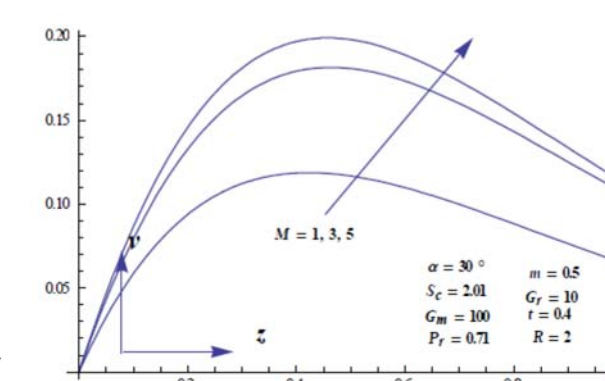


Figure 15. Velocity v for different values of M

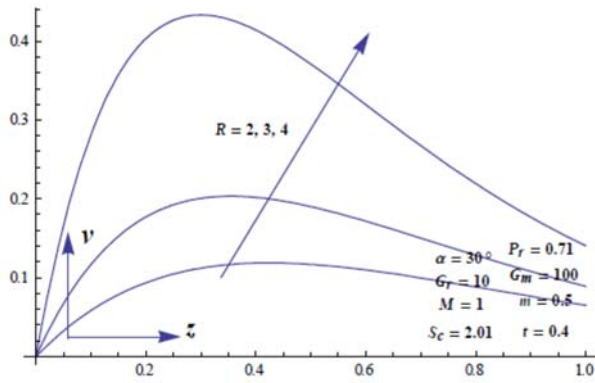


Figure16. Velocity v for different values of R

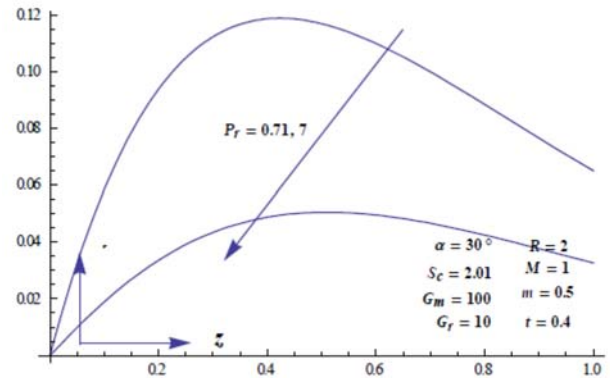


Figure 17. Velocity v for different values of Pr

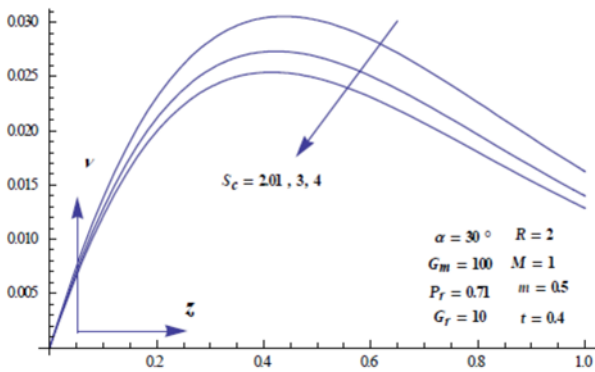


Figure18. Velocity v for different values of Sc

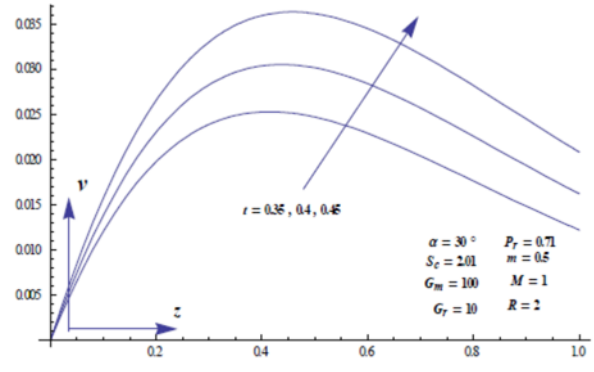


Figure 19. Velocity v for different values of t

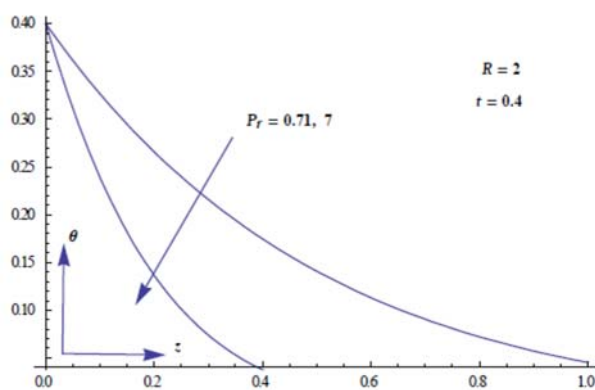


Figure 20. Temperature Profile for different values of Pr

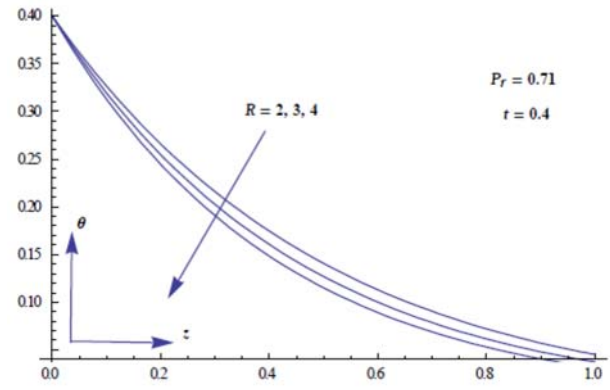


Figure 21. Temperature Profile for different values of R

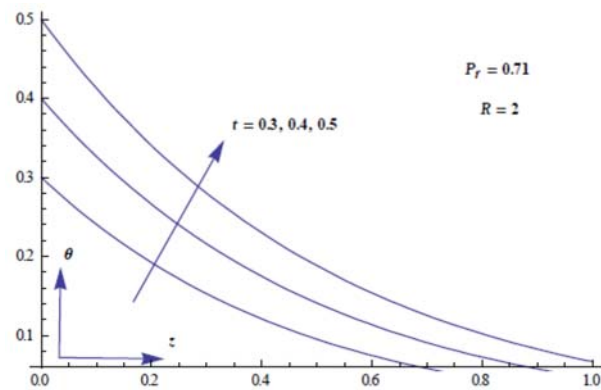


Figure 22. Temperature Profile for different values of t

Skin friction is given in Table 1. The value of τ_x increases with the increase in thermal Grashof number, mass Grashof Number, Hall current parameter, radiation parameter and time; and it decreases with the angle of inclination of plate, the magnetic field, Prandtl number and Schmidt number. Similar effects are observed with τ_y except magnetic field and Hall parameter, in which case τ_y increases with magnetic field parameter, and decreases with Hall parameter. Nusselt number is given in Table 2. The value of Nu decreases with increase in Prandtl number, radiation parameter and time.

Table 1. Skin friction for different parameters

α (in degrees)	M	m	Pr	Sc	Gm	Gr	R	t	τ_x	τ_y
15	2	1	0.71	2.01	100	10	2	0.2	8103.61	2130.75
30	2	1	0.71	2.01	100	10	2	0.2	7265.34	1910.40
60	2	1	0.71	2.01	100	10	2	0.2	4194.01	1103.07
30	3	1	0.71	2.01	100	10	2	0.2	6091.17	2319.00
30	5	1	0.71	2.01	100	10	2	0.2	4245.42	2518.92
30	2	3	0.71	2.01	100	10	2	0.2	9267.19	1576.14
30	2	5	0.71	2.01	100	10	2	0.2	9705.47	1066.28
30	2	1	7.00	2.01	100	10	2	0.2	-0284.03	3.42440
30	2	1	0.71	3.00	100	10	2	0.2	7265.07	1910.40
30	2	1	0.71	4.00	100	10	2	0.2	7264.89	1910.30
30	2	1	0.71	2.01	10	10	2	0.2	7263.21	1910.37
30	2	1	0.71	2.01	50	10	2	0.2	7264.16	1910.39
30	2	1	0.71	2.01	100	50	2	0.2	36323.3	9550.93
30	2	1	0.71	2.01	100	100	2	0.2	72645.7	19101.6
30	2	1	0.71	2.01	100	10	3	0.2	9450.92	2786.04
30	2	1	0.71	2.01	100	10	5	0.2	12657.8	4156.83
30	2	1	0.71	2.01	100	10	2	0.3	17285.2	7494.89
30	2	1	0.71	2.01	100	10	2	0.4	31655.0	20386.3

Table 2. Nusselt number for different parameters

Pr	R	t	Nu
0.71	2	0.4	-0.805273
7.00	2	0.4	-1.959260
0.71	3	0.4	-0.894014
0.71	4	0.4	-0.976083
0.71	2	0.5	-0.950956
0.71	2	0.6	-1.094940

4. Conclusion

In this paper a theoretical analysis has been done to study the unsteady MHD flow past an impulsively started inclined plate with variable temperature and mass diffusion in the presence of Hall current. The results obtained are in agreement with the usual flow. It has been found that the velocity in the boundary layer increases with the values of Hall current and radiation parameter. It is also observed that the Hall current and radiation parameter increases the skin friction. Further, the temperature of the fluid near the plate and the Nusselt number decrease with the increase in radiation parameter. The results of this paper may be useful to study some important flows like - plasma in MHD power generators, enhanced oil recovery and filtration systems etc.

References

- [1] Soundalgekar, V. M. and Takhar, H. S. 1993. Radiation effects on free convection flow past a semi-infinite vertical plate. *Modeling, Measurement and Control*, B, 51:31-40.
- [2] Watanabe, T. and Pop, I. 1995. Hall Effects on Magnetohydrodynamic Boundary Layer Flow over a Continuous Moving Flat Plate. *Acta Mechanica*, 108, 1: 35-47. doi: 10.1007/BF01177326.
- [3] Hossain, M.A. and Takhar, H. S. 1996. Radiation Effect on Mixed Convection along a Vertical Plate with Uniform Surface Temperature. *Heat and Mass Transfer*, 31, 4: 243-248. doi: 10.1007/BF02328616.
- [4] Takhar, H. S., Gorla, R.S., and Soundalgekar, V.M. 1996. Radiation Effects on MHD Free Convection Flow of a Radiating Gas past a Semi-Infinite Vertical Plate. *International Journal of Numerical Methods for Heat and Fluid Flow*, 6, 2: 77-83.
- [5] Raptis, A. and Massalas, C.V. 1998. Magnetohydrodynamics Flow past a Plate by the Presence of Radiation. *Heat and Mass Transfer*, 34, 2-3: 107-109. doi: 10.1007/s002310050237.
- [6] Raptis, A. and Perdikis, C. 1999. Radiation and Free Convection Flow past a Moving Plate. *Applied Mechanics and Engineering*, 4, 4: 817-821.
- [7] Chamkha, A. J., Takhar, H. S. and Bég, O. A. 2004. Radiative Free Convective Non-Newtonian Fluid Flow past a Wedge Embedded in a Porous Medium. *International Journal of Fluid Mechanics Research*, 31, 2:101 -115.
- [8] Mebine, P. 2007. Radiation Effects on MHD Couette Flow with Heat Transfer between Two Parallel Plates. *Global Journal of Pure and Applied Mathematics*, 3, 2: 191-202.
- [9] Hayat, T., Qasim, M. and Abbas, Z. 2010. Radiation and Mass Transfer Effects on the Magnetohydrodynamic Unsteady Flow Induced by a Stretching Sheet. *Zeitschrift für Naturforschung A*, 65, 3: 231-239. doi: 10.1515/zna-2010-0312.

- [10] Rajput, U. S. and Sahu, P. K. 2011. Combined Effects of MHD and Radiation on Unsteady Transient Free Convection Flow between Two Long Vertical Parallel Plates with Constant Temperature and Mass Diffusion. *General Mathematics Notes*, 6, 1: 25-39.
- [11] Rani, A. V. S., Sugunamma V., and Sandeep N. 2012. Hall Currents Effects on Convective Heat and Mass Transfer Flow of a Viscous Fluid in a Vertical Wavy Channel. *International Journal of Emerging trends in Engineering and Development*, 4, 2, 252-278.
- [12] Sandeep, N., Sugunamma, V., and Mohankrishna, P. 2014. Aligned Magnetic Field, Radiation, and Rotation Effects on Unsteady Hydromagnetic Free Convection Flow Past an Impulsively Moving Vertical Plate in a Porous Medium. *International Journal of Engineering Mathematics*, 2014, ID 565162 (7 Pages). doi: 10.1155/2014/565162.
- [13] Sandeep, N. and Sugunamma, V. 2014. Radiation and Inclined Magnetic Field Effects on Unsteady Hydromagnetic Free Convective Flow past an Impulsively Moving Vertical Plate in a Porous Medium. *Journal of Applied and Fluid Mechanics*, 7, 2, 275-286.
- [14] Azzam, G.E.A. 2002. Radiation Effects on the MHD Mixed Free-Forced Convection Flow Past a Semi-Infinite Moving Vertical Plate for High Temperature Differences. *Physica Scripta*, 66, 1: 71-76. doi: 10.1238/Physica.Regular.066a00071.
- [15] Muthucumaraswamy, R. and Kumar, G.S. 2004. Heat and Mass Transfer Effect on Moving Vertical Plate in the Presence of Thermal Radiation. *Theoretical and Applied Mechanics*, 31, 1: 35-46.
- [16] Muthucumaraswamy, R. and Janakiraman, B. 2006. MHD and Radiation Effects on Moving Isothermal Vertical Plate with Variable Mass Diffusion. *Theoretical and Applied Mechanics*, 33, 1: 17-29.
- [17] Prasad, V.R., Reddy, N.B., and Muthucumaraswamy, R. 2007. Radiation and Mass Transfer Effects on Two-Dimensional Flow past an Impulsively Started Infinite Vertical Plate. *International Journal of Thermal Sciences*, 46, 12: 1251 – 1258. doi: 10.1016/j.ijthermalsci.2007.01.004.
- [18] Rajput, U. S. and Kumar, S. 2013. Radiation Effect on MHD Flow through Porous Media past an Impulsively Started Vertical Plate with Variable Heat and Mass Transfer. *International Journal of Mathematical Archive*, 4, 10: 106-114.
- [19] Reddy, J. V. R., Sugunamma, V. and Sandeep, N. 2016. Thermo Diffusion and Hall Current Effects on an Unsteady Flow of a Nanofluid under the Influence of Inclined Magnetic Field. *International Journal of Engineering Research in Africa*, 20, 61-79. doi: 10.4028/www.scientific.net/JERA.20.61.

Appendix

$$A_1 = 1 + e^{2\sqrt{az}}(1 - A_{18}) - A_{17}, A_2 = -A_1, A_3 = 1 - e^{2\sqrt{az}}(1 - A_{18}) - A_{17}, A_4 = -1 + A_{19} + A_{30}(A_{20} - 1),$$

$$A_5 = -1 + A_{21} + A_{28}(A_{22} - 1), A_6 = -1 + A_{23} + A_{26}(A_{31} - 1), A_7 = -1 + A_{29} + A_{27}(A_{30} - 1),$$

$$A_8 = -1 + A_{23} + A_{26}(A_{31} - 1), A_9 = -1 - A_{24} - A_{28}(1 - A_{25}), A_{10} = -A_9, A_{11} = Abs[z].Abs[P_r],$$

$$A_{12} = e^{\frac{at}{P_r-1} - \frac{Rt}{P_r-1} - z} \sqrt{\frac{aP_r - R}{P_r - 1}}, A_{13} = e^{\frac{at}{S_c-1} - z} \sqrt{\frac{aS_c}{S_c - 1}}, A_{14} = e^{\frac{at}{P_r-1} - \frac{Rt}{P_r-1} - Abs[z]} \sqrt{\frac{P_r(aP_r - R)}{P_r - 1}},$$

$$\begin{aligned}
 A_{15} &= -1 + \operatorname{erf}\left[\frac{z\sqrt{S_c}}{2\sqrt{t}}\right], & A_{16} &= e^{Abs[z]\sqrt{P_r R}}, & A_{17} &= \operatorname{erf}\left[\frac{2\sqrt{at} - z}{2\sqrt{t}}\right], & A_{18} &= \operatorname{erf}\left[\frac{2\sqrt{at} + z}{2\sqrt{t}}\right], \\
 A_{19} &= \operatorname{erf}\left[\frac{z - 2t\sqrt{\frac{aP_r - R}{P_r - 1}}}{2t}\right], & A_{20} &= \operatorname{erf}\left[\frac{z + 2t\sqrt{\frac{aP_r - R}{P_r - 1}}}{2t}\right], & A_{21} &= \operatorname{erf}\left[\frac{z - 2t\sqrt{\frac{aS_c}{S_c - 1}}}{2t}\right], & A_{22} &= \operatorname{erf}\left[\frac{z + 2t\sqrt{\frac{aS_c}{S_c - 1}}}{2t}\right], \\
 A_{23} &= \operatorname{erf}\left[\frac{Abs[z].Abs[P_r]}{2\sqrt{t}} - \sqrt{\frac{tR}{P_r}}\right], & A_{24} &= \operatorname{erf}\left[\frac{2t\sqrt{\frac{a}{S_c - 1}} - 2\sqrt{S_c}}{2t}\right], & A_{25} &= \operatorname{erf}\left[\frac{2t\sqrt{\frac{a}{S_c - 1}} + 2\sqrt{S_c}}{2t}\right], \\
 A_{26} &= e^{2Abs[z]\sqrt{P_r R}}, & A_{27} &= e^{2Abs[z]\sqrt{\frac{P_r(aP_r - R)}{P_r - 1}}}, & A_{28} &= e^{-2z\sqrt{\frac{aS_c}{S_c - 1}}}, & A_{29} &= \operatorname{erf}\left[\frac{Abs[z].Abs[P_r]}{2\sqrt{t}} - \sqrt{\frac{t(R - aP_r)}{P_r(1 - P_r)}}\right], \\
 A_{30} &= e^{-2z\sqrt{\frac{aP_r - R}{P_r - 1}}}, & A_{31} &= \operatorname{erf}\left[\frac{Abs[z].Abs[P_r]}{2\sqrt{t}} + \sqrt{\frac{tR}{P_r}}\right], & A_{32} &= \operatorname{erf}\left[\frac{Abs[z].Abs[P_r]}{2\sqrt{t}} + \sqrt{\frac{t(R - aP_r)}{P_r(1 - P_r)}}\right], \\
 A_{33} &= 1 + A_{17} + e^{2\sqrt{a}z}A_{34}, & A_{34} &= \operatorname{erfd}\left[\frac{2\sqrt{at} + z}{2\sqrt{t}}\right],
 \end{aligned}$$